Chemical Engineering Journal 528 (2026) 172380

Contents lists available at ScienceDirect

Chemical Engineering Journal

journal homepage: www.elsevier.com/locate/cej

Customizing bioelectrochemical ammonium recovery: towards application-specific effluents

David Fernández-Verdejo [a], Mariella Belén Galeano [a], Zainab Ul [a], Deepak Pant [b,c], Juan Antonio Baeza [a,*], Albert Guisasola [a]

[a] GENOCOV, Departament d'Enginyeria Química, Biològica i Ambiental, Escola d'Enginyeria, Universitat Autònoma de Barcelona, 08193 Bellaterra (Cerdanyola del Vallès), Barcelona, Spain
[b] Electrochemistry Excellence Centre (ELEC), Materials & Chemistry Unit, Flemish Institute for Technological Research (VITO), Boeretang 200, 2400, Mol, Belgium
[c] Centre for Advanced Process Technology for Urban Resource Recovery (CAPTURE), Frieda Sayesstraat 1, Zwijnaarde, 9052, Belgium

ARTICLE INFO

Keywords:
Ammonium recovery
Bioelectrochemistry
Effluent characterization
Gas diffusion electrode
Komagataella phaffii
Microbial electrolysis cell

ABSTRACT

Ammonium recovery from wastewater is of increasing interest due to its environmental implications and potential economic and energy benefits. In this study, a three-chamber bioelectrochemical system (BES) incorporating nickel-based gas diffusion electrodes was operated in continuous mode, achieving high ammonium recovery rates (47 g NH_4^+-N/m^2/d) and current densities (3.6 A/m^2), with low energy requirements (~ 1.0 kWh/kg NH_4^+-N recovered). The established biofilms and membrane materials maintained stable performance over extended operation (>80 d). The effects of recovery solution flow rate (40, 60 and 83 mL/d) and acid type (sulfuric, phosphoric and nitric) on effluent quality were systematically evaluated. For each condition, the properties of the recovered effluent regarding pH (ranging between 1 and 10) and ammonium concentration (from 2.8 to 11.0 g NH_4^+-N/L) were evaluated, providing a flexible platform for generating application-specific ammonium solutions. All tested conditions delivered competitive nitrogen recovery rates (>29 g NH_4^+-N/m^2/d), with several scenarios outperforming previous BES configurations. The recovered effluents were validated as a nitrogen source in *Komagataella phaffii* fermentation, achieving 3-hydroxypropionic acid concentrations 7 % higher than those obtained when using a commercial ammonium source.

1. Introduction

Ammonium, a frequently found compound in industrial wastewater, can contribute to the eutrophication of natural water sources [1]. Its removal has been extensively studied using biological (e.g., nitrification/denitrification) or abiotic methods, such as air stripping, precipitation, or reverse osmosis. The major advantage of the latter methods is that ammonium can be recovered rather than transformed into another N-species. However, they are energy-intensive technologies and may require the application of additional chemicals, hindering their environmental sustainability [2,3]. Ammonium recovery holds both energetic and economical interest, as it can be used as fertiliser, fuel, or an efficient hydrogen carrier [4,5]. The Haber-Bosch process currently employed for ammonium production is, nowadays, responsible for 2 % of the world's total energy consumption and more than 1 % of global CO_2 emissions [6]. Ammonium can outcompete nitrate as fertiliser and, additionally, ammonium has a lot of interest in the biotechnological industry as it is commonly found as a strict requirement in several defined media for growing microorganisms [7,8].

In recent years, bioelectrochemical systems (BES) have emerged as a promising alternative for recovering the total ammoniacal nitrogen (TAN) from wastewaters in the context of the circular economy [9]. Typically, in a BES, the driving force behind the ammonium transport is the charge imbalance created by the electric current between the anode and the cathode, which allows the transfer of positive charges through the cationic exchange membrane (CEM) that separates the anolyte and the catholyte [10].

In conventional electrochemical systems, the driving force for this electron flow between both electrodes can be supplied entirely by an external current source. However, in BES, the external energy requirements are lowered due to the presence of anode-respiring bacteria (ARB) that can oxidise organic matter using the anode as an electron acceptor [11,12]. Thus, BES require milder conditions than conventional electrochemical systems in terms of medium composition, pH, and

* Corresponding author.
E-mail address: JuanAntonio.Baeza@uab.cat (J.A. Baeza).

https://doi.org/10.1016/j.cej.2025.172380
Received 27 August 2025; Received in revised form 7 November 2025; Accepted 27 December 2025
Available online 29 December 2025

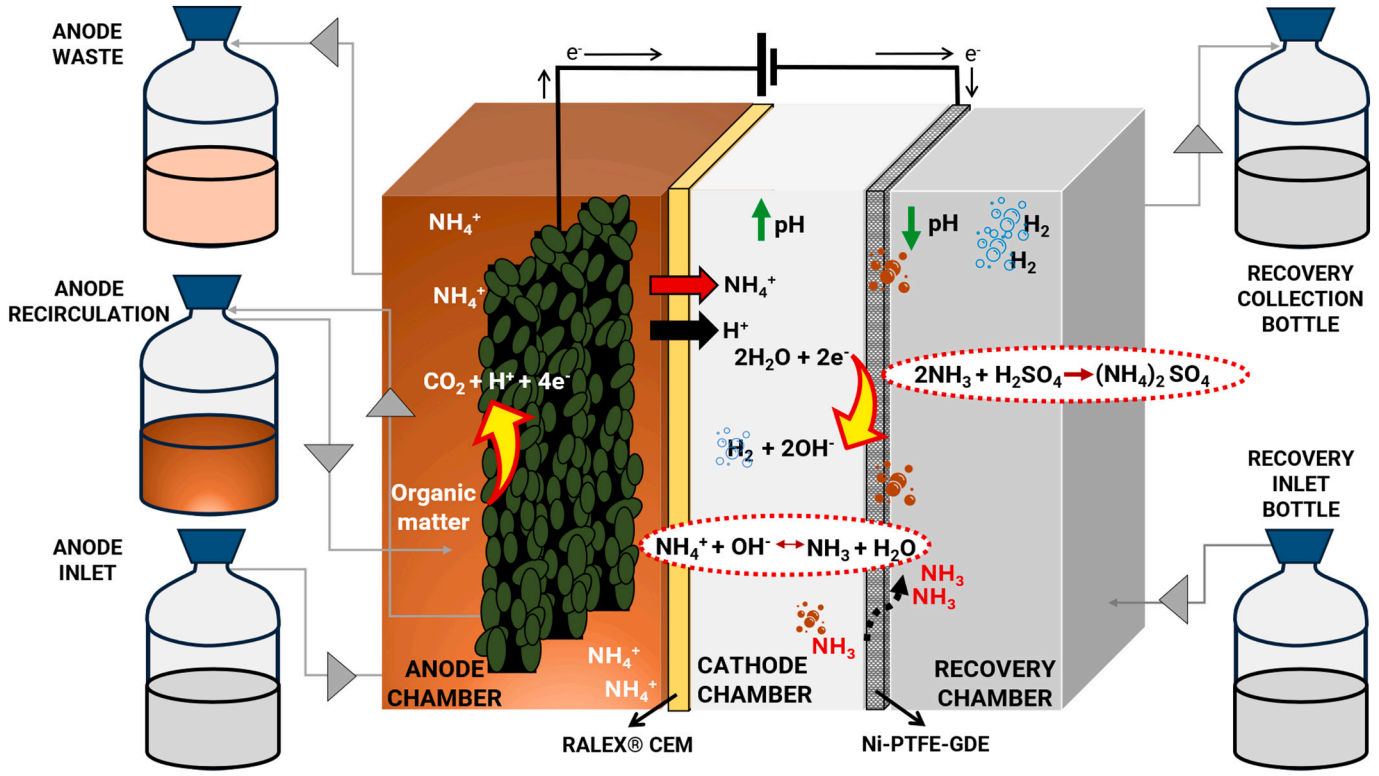

Fig. 1. Scheme of the three-chamber bioelectrochemical setup for TAN recovery.

current densities compared to their abiotic counterparts [13]. These restrictions bring a lower performance in terms of TAN transfer rates, but, simultaneously, can vastly improve the energetic efficiency of the process, especially if the external carbon source added as substrate is a waste.

There are two main types of BES that enable electrochemical ammonium recovery. In microbial fuel cells (MFCs), the cathodic reaction is oxygen reduction, the electron flow from the anode to the cathode is spontaneous, and electrical energy is produced simultaneously to the ammonium transfer. On the other hand, when hydrogen evolution reaction (HER) is the cathodic reaction, an external energy supply is required and the systems are described as microbial electrolysis cells (MECs) [14,15]. MFCs are by far the most energetically efficient system, as they have a net energy gain at the expense of providing low currents and low TAN recovery performances [16]. MECs provide better performances at a reasonable energetic efficiency due to the moderate external current supplied, making it the most studied configuration [17–21]. Furthermore, MECs could compensate for the external energy supply by recovering the hydrogen produced in the cathode [22]. Several studies treating wastewater, even at higher scales, have reported energetic sustainability when operating in MEC configuration [23].

Key performance indices are the TAN recovery rate and also the properties (pH and concentration) of the recovered ammonium-enriched effluent. Moreover, the concentration gradient at both sides of the CEM is a key parameter in the cation transfer rate between anode and cathode. The transfer of ammonium can, thus, be hindered by other cations, such as sodium or potassium [24]. Consequently, it is preferable to remove TAN from the catholyte and accumulate it in an external vessel to minimize the negative effects of possible concentration gradients. Several methodologies for removing the ammonium from the catholyte have been proposed, including using air stripping or employing a transmembrane chemisorption process to transfer TAN to an adjacent chamber [17,25,26].

The chemical properties of ammonium, coupled with the nature of a dual-chamber BES, make transmembrane chemisorption an interesting approach for TAN recovery [27]. When hydrogen is produced at the cathode, the cathodic pH increases to very alkaline levels. Several electrode materials based on noble and non-noble metals have been tested [28] to drive these reactions. The latter are more suitable due to their lower cost compared to the noble metals. Among them (e.g. cobalt, iron or molybdenum), nickel stands out due to its balance between good performance, low cost and high durability, while also being the most suitable for operating in alkaline conditions as the ones found in the catholyte. These high pH values promote the conversion of TAN into ammonia (the pKa of ammonium is 9.25 at 25 °C). Thus, ammonia can cross a hydrophobic membrane and reach a third chamber, commonly filled with an acidic solution for its recovery. The recovery effluent would be a concentrated solution of ammonium with the anion corresponding to the employed acid. Besides, employing membranes to remove the TAN from the cathode can also potentially improve the scalability of the process by avoiding the high costs involved in aeration during a stripping process [29]. Among other employed materials such as polypropylene (PP) or polyvinylidene fluoride (PVDF), polytetrafluoroethylene (PTFE) is highly valued due to its chemical inertness, thermal and mechanical stabilities, low permeability and electrical insulation [30].

Despite the general focus in the literature on using the recovered TAN mainly as fertiliser, high and pure ammonium salt effluents can be used also as nutrient source in biotechnological processes, for instance aiming at the production of added value compounds [29,31]. However, most reports focus on maximizing TAN recovery values and do not properly characterize the properties of the achieved effluent in view of real-world applications of the collected ammonium-enriched solution. This narrow approach to TAN recovery creates a gap between research and the practical application of these systems.

In recent years, novel membrane assemblies combining an electrode and a hydrophobic membrane, known as gas diffusion electrodes (GDEs), have been studied for TAN recovery [18,32]. Due to their ambivalent hydrophilic and hydrophobic nature, GDEs enable the ammonium present in the catholyte to get closer to the metallic

hydrophilic layer acting as the electrode, favouring the creation of a local gradient of high pH, which promotes the conversion to ammonia. The membrane assembly configuration of the GDE facilitates that ammonia is produced in the vicinity of the hydrophobic membrane and, hence, its transfer to the recovery chamber while preventing the interference of other cations. Moreover, GDEs employed as cathodes can be fabricated at low cost and have been observed to repel negatively-charged foulants, solving one of the main limitations of the transmembrane chemical adsorption methodology and consequently improving the average lifetime of the hydrophobic membranes [27,33].

The aim of this study is to examine the impact of various operational parameters on the performance of a three-chamber BES with a GDE over extended periods. The properties of the ammonium-enriched effluent are evaluated with the aim of maximizing ammonium recovery rate and minimizing energetic consumption, by testing various recovery solution compositions and flowrates. Additionally, the stability of the system is evaluated during long-term operation without replacing the membranes or electrodes. In order to test the validity of the recovered ammonium-enriched effluent, several of the previous outlet streams are employed as nutrient sources to produce 3-hydroxypropionic (3-HP) as a model added-value compound in a *Komagataella phaffii* fermentation. These results aim to demonstrate, for the first time, the production of high added-value products using as nitrogen source custom-made ammonium-enriched recovered effluents from a three-chamber BES.

2. Materials and methods

2.1. BES setup

The three-chamber bioelectrochemical systems (3C-BES, Figs. 1 and S1) employed are similar to those used in a previous work [17,25]. In brief, the 3C-BES were composed of three chambers, acting respectively as anode (0.4 L), cathode (0.2 L) and recovery (0.2 L), with a cross-sectional area of 0.01 m^2. A CEM (RALEX® CMH-PP 840 mm, Mega, Czech Republic) was employed as a separator between the anolyte and the catholyte. A PTFE and nickel-based GDE (VITO CORE®) was employed as both cathode and separator between the catholyte and the recovery solution. Cathodes were fabricated at VITO (Belgium) by compressing a blend of activated carbon (AC; 70–90 wt%, Norit SX Plus, Norit Americas Inc., TX) and PTFE binder onto a nickel mesh current collector (#53 mesh, 330 μm opening, 150 μm wire diameter) at a pressure of 150 bar [34]. Simultaneously, three graphite brushes (75 mm length × 50 mm diameter, fiber diameter of 7.2 μm, Millrose Co., USA) were employed in the anodic chamber as anodes. This chamber was hydraulically connected to an external vessel (0.5 L) resulting in a total anolyte volume of 0.9 L. Both the anodic and recovery chambers had inlet and outlet ports to apply a continuous flowrate when required. All flowrates are reported as measured on the collected effluent volumes in time. The anolyte was continuously recycled (100 mL/min) between the anodic chamber and the external vessel. A TEDLAR gas bag was located on top of the recovery chamber to collect the gases (produced at the cathode and transferred to the recovery chamber) to avoid overpressure.

A power source (Programmable DC LAB Power supply LABPS3005DN, Velleman Group, Belgium) was used to apply a voltage of 1 V between anode and cathode. The measure of the voltage at both sides of an external resistor (10 Ω) located at the anodic connection was employed to monitor the current intensity (every 10 min) thanks to a 16-bit data acquisition card (Advantech PCI-1716) operated with Add-Control software, developed by the GENOCOV research group in LabWindows CVI [35].

2.2. Media and operation of the BES

The anolyte and the catholyte of the BES were composed of a synthetic wastewater containing (per litre) 1.5 g $NaHCO_3$, 300 mg K_2HPO_4, 100 mg $MgSO_4{\cdot}6H_2O$ and 50 mg $CaCl_2$. Additionally, the anolyte also included 28.5 g/L of NH_4HCO_3; which accounted to 5.1 g of NH_4^+-N/L; and 5 g/L of CH_3COONa as ammonium and carbon sources, respectively. On the other hand, the recovery chamber was filled with an aqueous solution of the corresponding acid (sulfuric, phosphoric, or nitric acids) at the concentrations stated at each experiment. To ensure replicability, all conditions were tested in two parallel reactors.

At the start of the operation, before starting the peristaltic pumps, each reactor vessel was filled with their corresponding solution, which had the same composition than their reactor counterparts. The catholyte was not added nor removed after starting the operation. Previously to the operation, the anodes had been inoculated in the same systems with anaerobic sludge collected at a wastewater treatment plant. During the inoculation period, which lasted between 2 and 4 weeks, the anodic chamber operated in batch mode with several doses of acetate (1 g/L) and permanent high ammonium concentrations (>1 g NH_4^+-N/L) until consistent intensities were achieved. An individual feed condition was maintained until a pseudo steady state was reached (between 4 and 10 days).

2.3. Chemical analysis

Ammonium was measured by employing a Dionex DX120 ion chromatograph with AS40 autosampler, a Dionex IonPac CS16 cation exchange column and 38 mM methanesulfonic acid as the eluent at a flowrate of 1 mL/min. Anions (sulphate, phosphate and nitrate) were monitored with an ion chromatograph as described elsewhere [36]. Both samples were previously filtered by employing a 0.22 μm PTFE filter (VWR, Amsterdam, The Netherlands). The pH of each sample was measured with a pH probe (HACH pH electrode, Crison5233, Spain) and for the conductivity a conductivity meter (COND 8, XS Instruments, Italy) was employed.

2.4. Calculations

Ammonium removal, in terms of efficiency (E_{rem}, %, Eq. (1)) and rate (R_{rem}, g NH_4^+-N/m^2/d, Eq. (2)), refers to the amount of TAN eliminated in the anode normalized by the anodic and cathodic effective surface areas (0.01 m^2), and was calculated as described elsewhere [17]:

$$E_{rem}(\%) = \frac{NH_4^+ - N_{inlet\ an} - NH_4^+ - N_{outlet\ an}}{NH_4^+ - N_{inlet\ an}} \cdot 100 \quad (1)$$

where $NH_4^+ - N_{\text{inlet an}}$ and $NH_4^+ - N_{\text{outlet an}}$ are the TAN concentrations in the anodic inlet and the outlet (g/L).

$$R_{rem} = \frac{\left(NH_4^+ - N_{inlet\ an} - NH_4^+ - N_{outlet\ an}\right) \cdot V_{an}}{A \cdot t} \quad (2)$$

where V_{an} is the volume of anolyte treated (L), A is the electrodes projected surface area (m^2) and t is the operational period of time (d).

Ammonium recovery, in terms of efficiency (E_{rec}, %) and rate (R_{rec}, g NH_4^+-N/m^2/d), refers to the amount of TAN present in the recovery effluent. E_{rec} (Eq. (3)) correlates the amount of ammonium collected in the recovery solution compared to the amount removed at the anode:

$$E_{rec}(\%) = \frac{NH_4^+ - N_{outlet\ rec} \cdot V_{rec}}{\left(NH_4^+ - N_{inlet\ an} - NH_4^+ - N_{outlet\ an}\right) \cdot V_{an}} \cdot 100 \quad (3)$$

where $NH_4^+ - N_{\text{outlet rec}}$ is the TAN concentration in the recovery effluent (g/L) and V_{rec} is the volume of collected recovery solution (L).

R_{rec} (Eq. (4)) is the rate of ammonium recovered:

$$R_{rec} = \frac{NH_4^+ - N_{outlet\ rec} \cdot V_{rec}}{A \cdot t} \quad (4)$$

The global efficiency (E_{glo}, %) combines the removal and the recovery and correlates the amount of ammonium recovered with the one

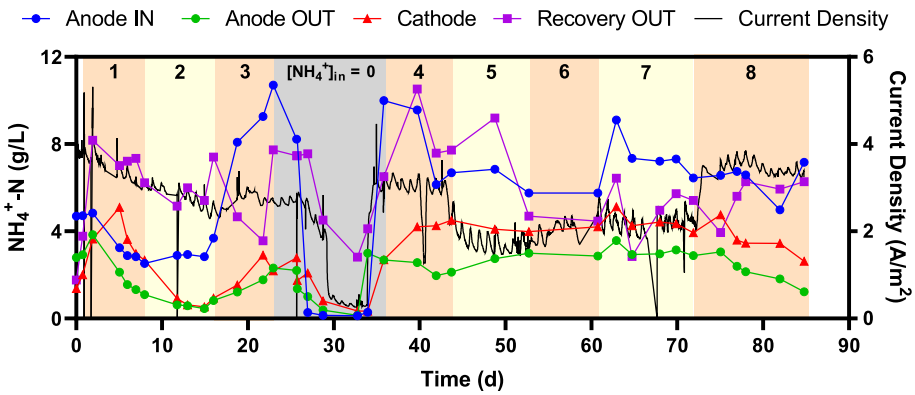

Fig. 2. TAN concentration at each reactor chamber (anode inlet, anode outlet, cathode, and recovery outlet) and current density during a continuous-flow BES operation, for each experimental period 1 to 8.

being introduced into the system through the anolyte (Eq. (5)):

$$E_{glo}(\%) = \frac{E_{rem} \cdot E_{rec}}{100} \quad (5)$$

The current densities were also standardized by employing the projected surface areas. The voltage applied in each reactor (V_{ap}, V) was calculated in Eq. (6), where V_{pow} is the voltage set up in the power source (1 V) and V_{res} is the voltage lost in the 10 Ω resistor (V):

$$V_{ap} = V_{pow} - V_{res} \quad (6)$$

The energy consumption for ammonium removal (W_{rem}, kWh/kg $NH_4^+ - N$) was calculated in Eq. (7):

$$W_{rem} = \frac{\int I \cdot V_{ap} \; dt}{\left(NH_4^+ - N_{inlet\ an} - NH_4^+ - N_{outlet\ an}\right) \cdot V_{an}} \quad (7)$$

where $\int(I \cdot V_{ap})dt$ is the integration of the product between the monitored intensity and the applied voltage (kWh).

Similarly, the energy consumption for ammonium recovery (W_{rec}, kWh/kg $NH_4^+ - N$) was calculated with Eq. (8):

$$W_{rec} = \frac{\int I \cdot V_{ap} \; dt}{NH_4^+ - N_{outlet\ rec} \cdot V_{rec}} \quad (8)$$

The ammonium transport number through the CEM (t_N, %), which correlates the ammonium removed from the anode with the amount of electrochemically transferred charge in the system, was calculated with Eq. (9) [37]:

$$t_N(\%) = \frac{\left(NH_4^+ - N_{inlet\ an} - NH_4^+ - N_{outlet\ an}\right) \cdot V_{an} \cdot F}{M_N \cdot \int Idt} \cdot 100 \quad (9)$$

where F is the Faraday constant (96,485.34 C/mol electrons), M_N is the molar mass of nitrogen (14 g/mol), and $\int Idt$ is the integration of the monitored intensity (C).

The ammonium loading ratio (L_R, %) correlates the electrical charge through the system with the amount of ammonium input in the anodic chamber, and was calculated with Eq. (10) [12]:

$$L_R(\%) = \frac{M_N \cdot \int Idt}{NH_4^+ - N_{inlet\ an} \cdot V_{an} \cdot F} \cdot 100 \quad (10)$$

2.5. Statistical analysis

All statistical analyses were performed with GraphPad Prism 8 software. For bar figures, statistical analyses comprised a two-way analysis of variance (ANOVA) test with a Tukey's multiple comparison test to assess differences in the results for the different operating conditions. Statistical significance was considered at $p < 0.05$. For boxplot figures, statistical analyses comprised a two-way ANOVA with Brown–Forsythe and Welch corrections to account for potential differences in variance between groups. Statistical significance was considered at $p < 0.05$.

2.6. Fermentation with K. phaffii

To assess the potential of BES-recovered ammonium sulphate and ammonium phosphate as nitrogen sources, *K. phaffii* fermentations were conducted targeting 3-HP production. *K. phaffii* strain was inoculated from cryovial into 10 mL YPD (10 g/L yeast extract, 20 g/L peptone, 20 g/L glucose) medium in 50 mL falcon tubes. Cultures were grown overnight at 30 °C and 180 rpm. The overnight cultures were then diluted to an OD600 of 0.2 in 1 L shake flasks containing YNB medium and grown in an orbital incubator for 48 h at 28 °C and 180 rpm. Samples were taken during the experiment to measure the OD600 using a Lange DR 3900 spectrophotometer (Hach, Loveland, CO, USA).

The yeast nitrogen base (YNB) medium used for growth contained per litre: 2 µg of biotin, 2 µg of folic acid, 40 µg of copper sulphate, 400 µg of calcium pantothenate, 400 µg of niacin, 200 µg of P-aminobenzoic acid, 400 µg of pyridoxine hydrochloride, 200 µg of riboflavin, 400 µg of thiamine, 500 µg of boric acid, 100 µg of potassium iodide, 200 µg of ferric chloride, 400 µg of manganese sulphate, 200 µg of sodium molybdate, 400 µg of zinc sulphate, 2000 µg of inositol, 0.5 g of potassium dihydrogen phosphate, 250 mg of magnesium sulphate, 50 mg of sodium chloride and 50 mg of calcium chloride. YNB medium was sterilized by filtration with a 0.2 µm pore size single-use syringe filter (SLLGX13NK, Merck Millipore, CA, USA) before its subsequent usage. All sets of experiments contained the same amount of ammonium concentration (2.5 g), which was obtained from autoclaved BES effluents. The pH was adjusted to 5 using 5 M HCl. Each shake flask contained 100 mL of YNB medium. Each fermentation experiment was identical in all aspects other than the nitrogen source. Methanol was used as the carbon source. The performance was assessed by monitoring optical density, methanol consumption, and 3-HP concentration across all conditions.

Two set of experiments were performed. In the first experiment, duplicate shake flasks were used to test ammonium sulphate from three different sources: controls with commercial ammonium sulphate and BES-recovered ammonium sulphate collected at pH 2.1 and 8.8. The second experiment followed a similar design, employing duplicates with a 50–50 mix of ammonium from recovered ammonium sulphate and ammonium phosphate, tested both with and without added potassium as KCl (0.27 g), along with controls using commercial ammonium sulphate. The final mixture pH for every experiment was manually adjusted to 5 before starting the fermentation.

Table 1
Summary of recent studies concerning (bio)electrochemical recovery of TAN.

Treated influent	System	Cathode material	V_{ap} (V)	Current density (A/m^2)	R_{rem} (g NH_4^+-N /m^2/d)	R_{rec} (g NH_4^+-N /m^2/d)	W_{rem} (kWh/kg NH_4^+-N)	W_{rec} (kWh/kg NH_4^+-N)	Study
Synthetic wastewater	Three-chamber BES with TCMS	Nickel and PTFE GDE	0.75 ± 0.05	2.45 ± 0.54	44.5 ± 12.0	47.0 ± 12.5	1.06 ± 0.13	1.00 ± 0.03	This study
Synthetic wastewater	Three-chamber BES with TCMS	Stainless steel	1.4	3.8	52	33	2.7	4.5	Previous study [17]
Synthetic wastewater	Three-chamber BES with TCMS	Nickel foam	1.4	3.3	35	25	2.0	5.2	Previous study [17]
Synthetic medium	Three-chamber BES with TCMS	Nickel and polypropylene GDE	0.8	3.0	n.r.	36.2 ± 1.2	n.r.	1.61 ± 0.03	[18]
Digestate	Three-chamber BES with TCMS	Stainless steel mesh	Poised anode (0 mV vs Ag/AgCl electrode)	1.40 ± 0.71	81.6 ± 28.8	36.0 ± 19.2	n.r.	n.r.	[19]
Synthetic blackwater	Two-chamber BES with stripping	Carbon fiber and polyethylene GDE	0.2	2.5 ± 0.2	15.8 ± 1.6	9.6 ± 1.9	1.6	2.2	[21]
Synthetic blackwater	Single-chamber BES with TCMS and void pumping	Carbon black and PTFE GDE	0.8	16.7 ± 2	n.r.	178	n.r.	2.41	[32]
Synthetic medium	Two-chamber electrochemical system with TCMS	Carbon cloth and polypropylene GDE	n.r.	62.5	n.r.	141 ± 14	n.r.	69.2 ± 5.3	[39]
Livestock wastewater	Two-chamber electrochemical system with TCMS and stripping	Platinum GDE	n.r.	100	n.r.	770	n.r.	9.44	[26]

TCMS: transmembrane chemisorption, n.r.: not reported.

3. Results and discussion

3.1. Bioelectrochemical ammonium recovery as ammonium sulphate

A continuous 3C-BES was operated during 8 experimental periods, each corresponding to a different batch of anodic inlet feed (blue dots in Fig. 2). The flowrates for the anode and recovery chambers were 100 and 83 mL/d respectively, corresponding to hydraulic retention times of 9.0 and 2.4 days. On the opposite side of the cell, a concentration of 0.187 M of sulfuric acid was used in the recovery solution. The anodic biofilm, having been previously acclimated to high ammonium concentrations, was able to successfully deliver current density values higher than 3 A/m^2 when the influent contained a TAN concentration of 5 g/L. When fed with acetate, the coulombic efficiency in these systems fluctuates between 70 and 80 % [17].

The first experimental period, i.e., the start-up period, lasted 8 days. Average removal efficiency (E_{rem}) was 36 % while the TAN cathodic and recovery concentrations increased. In the two subsequent periods (2 and 3), E_{rem} increased to values higher than 70 % (Table S1) and the recovery rates (R_{rec}) escalated up to 47 and 42 g NH_4^+-N/m^2/d, which are among the highest reported in the literature for ammonium recovery employing BES [9]. The direct cause behind these high R_{rec} was the high current intensities produced by the anodic biofilm (3–4 A/m^2), which was in the higher range among the values commonly reported for BES employed in ammonium recovery [18,19]. The charge gradient caused by the electron flow from anode to cathode enabled the ammonium transport between both chambers through the CEM. Subsequently, the pH values achieved in the cathodic vessel (9.4–10.1) promoted the conversion of the soluble ammonium cations into ammonia, which could cross the GDE and reach the sulfuric acid solution in the recovery chamber.

After the third period, the system was subjected to a period of 10 days without external TAN inlet to assess the adaptation capability of the anodic biofilm to variable anodic TAN and conductivity inlet conditions. The inlet still contained enough organic matter for the exoelectrogens to survive. After 4 days of operation, 83 % decrease in the monitored intensity was observed due to the lower conductivity of the reactor caused by the absence of TAN in the inlet. During the first three periods, the ammonium hydrogen carbonate salt represented 93 % of the total conductivity in synthetic wastewater (from 27 to 2 mS/cm for the anode inlet with and without ammonium salt respectively). Moreover, it has been previously reported that the presence of TAN increases the permeability of the bacterial membrane, maximizing the exoelectrogenic activity [38]. Hence, TAN presence was proven to be beneficial for the bioelectrochemical performance. However, this positive effect should be taken with care since high TAN concentrations are reported to be inhibitory to biological systems. Thus, if the biofilm tolerates such high concentrations (for instance, through a stepwise adaptation strategy), increased TAN levels may enhance system performance by augmenting conductivity.

During the 4th period, the system was fed again with the N-concentrated synthetic wastewater (7 g NH_4^+-N/L) and the previous current densities were recovered, revealing the resilience of the anodic biofilm. The BES was subsequently operated during 5 additional experimental periods, each one corresponding to a new batch of feeding solution, achieving removal and recovery performances similar to those in periods 2 and 3.

A major outcome of this work was that the system was able to operate under similar conditions in a long-term basis. No apparent deterioration in the performance of each critical reactor component (anode, GDE or CEM) was observed during the close to 90-days operation, demonstrating that both, physical materials and the biofilm, could sustain continuous operation during long time spans.

Table 1 summarises the average steady-state performance values for periods 3 to 8, together with the results of a parallel reactor operating under the same conditions (Fig. S2). These performance values are compared to our own previous values achieved with the same systems working under a non-GDE cathodic configuration. Stainless steel (SS) or nickel foam (NF) were used as cathode and they were coupled to an independent hydrophobic membrane acting as separator [17]. In this previous work, a voltage of 1.4 V was applied, notably higher than the 0.75 ± 0.05 V averaged in the selected periods of our GDE operation. The lower voltage poised in the current study resulted only in a decrease of 36 % and 26 % in the observed current densities compared to the experiments with SS and NF respectively.

The loading ratio (L_N) was calculated for this period as 45 ± 13 % (Eq. (10)). This indicates that with this current density and with such high inlet TAN load, the system can only transport approximately half of

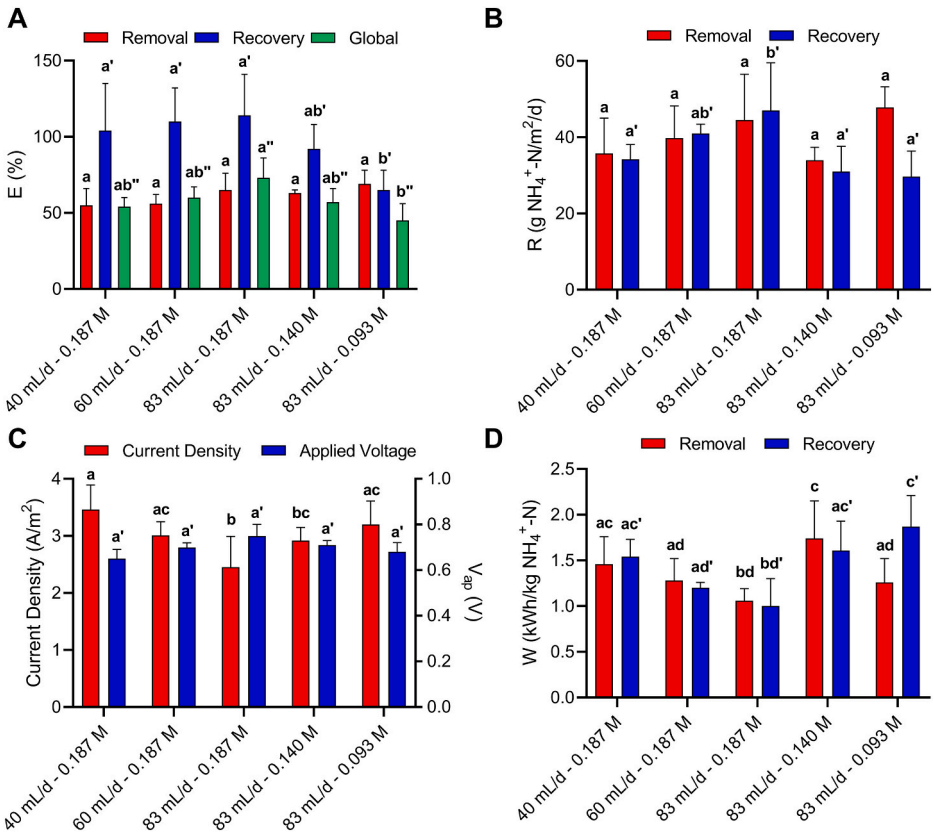

Fig. 3. Summary of values achieved during the recovery of ammonium testing different sulfuric acid concentrations and flowrates in the recovery solution: E_{rem}, E_{rec} (A), R_{rem}, R_{rec} (B), current density, V_{ap} (C), W_{rem} and W_{rec} (D). Colour bars represent average values of all the selected experimental periods, error bars represent the standard deviation and different letters above bars indicate significant differences among treatments according to Tukey's test ($p < 0.05$). The number of selected experimental periods for each condition was: 40 mL/d – 0.187 M = 6, 60 mL/d – 0.187 M = 7, 83 mL/d – 0.187 M = 9, 83 mL/d – 0.140 M = 4 and 83 mL/d – 0.093 M = 7.

the entering ammonium. Higher current density values are required to transport all the ammonium entering in the system. Similarly, the ammonium removal performance achieved in this work resulted in high ammonium transport number (t_N) of 139 ± 30 %. This high value indicates that the amount of TAN transferred through the membrane to the cathode was higher than to the number of electrons flowing from the anode to the cathode. Thus, diffusion also played an important role in the TAN transport through the CEM [20].

The nickel-based GDE configuration showed lower current density that those with electrode+separator. However, R_{rem} was 27 % higher than that with NF electrode+separator. Nevertheless, R_{rem} was still 14 % lower than those with SS electrode+separator due to the much higher current densities achieved in that work. In any case, the main benefit of the nickel-based GDE configuration lays on the lower V_{ap} and current density values achieved, which result in a 50 % decrease of the energy used per kg of TAN removed (W_{rem}). This improvement in the energetic efficiency could be [29] also attributed to the lower electrical resistance offered by the CMH-PP RALEX CEM installed in this reactor compared to the CMI-7000 (Membrane International, Membranes International, Inc., Ringwood, NJ, USA) used in our previous studies [10].

Table 1 shows that replacing the electrode+separator configuration for a GDE increased the R_{rec} by 42 % and 88 % regarding the SS and NF electrodes, respectively. While operating with GDE, the R_{rem} and R_{rec} were found to be approximately equivalent (indicating no TAN loss/accumulation in the system). In previous works, the E_{rec} attained in the SS and NF systems was lower (63 % and 71 %, respectively). N-species accumulated in the cathodic chamber and suggested that the most limiting transport step was the hydrophobic membrane resistance between cathode and recovery chambers. On the other hand, the application of a GDE led to a steady state where the same amount of TAN was transported through the CEM between anode and cathode and through the GDE between cathode and recovery. The transport of TAN through the hydrophobic membrane is highly dependent in its conversion into ammonia which is promoted at high pH [18]. The GDE configuration (i.e. merging electrode and hydrophobic layer) promotes a high local pH in the vicinity of the membrane and also the electroadsorption reaction of ammonium ions. Both aspects promoted the conversion of ammonium into ammonia and, thus, the TAN transfer. This bonus combination would not occur when conventional electrodes were positioned at a certain distance from the hydrophobic membrane. Moreover, the continuous flow in the recovery chamber can avoid the undesired accumulation of TAN in the acidic solution. This accumulation would hinder the mass transfer from the cathode to the recovery chamber.

The R_{rec} values consistently achieved in this reactor, despite the long uninterrupted operational time, are among the highest ones reported in the literature so far for BESs recovering TAN [18,19,21]. The only BES report with higher R_{rec} (178 g NH_4^+-N/m^2/d) also employed a BES with a GDE as cathode [32]. In this case, the system worked in batch mode, the surface area was smaller (58 cm^2), the recovery system employed underpressure conditions and both, catholyte and cathodic GDE, were restored every 12 h. R_{rec} are higher but some of these strategies are difficult to be scaled-up.

Furthermore, the high rates achieved in our system while applying relatively low voltages obtained the lowest energetic input reported, W_{rec}, of 1.00 ± 0.03 kWh/kg NH_4^+-N recovered. This value is 78 % and 81 % lower than those obtained with our previous configurations with SS and NF, respectively and much lower than those reported for other

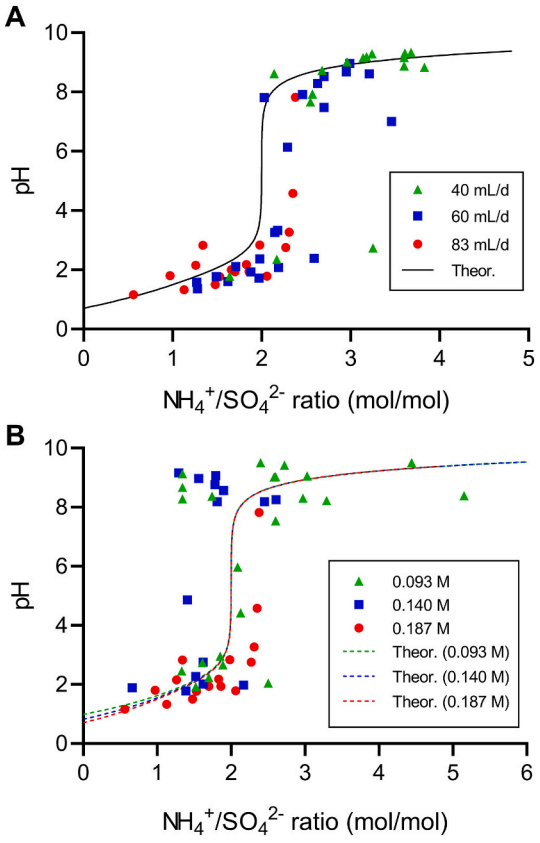

Fig. 4. pH of the recovery solution as a function of the molar ratio of NH_4^+/SO_4^{2-} for each datapoint of the experiments testing different sulfuric acid flowrates (A) and concentrations (B) of the acidic solution of the recovery chamber, compared to the theoretical values.

biological systems. On the other hand, as expected, R_{rec} values higher than 100 g NH_4^+-N/m^2/d are reported for abiotic electrochemical systems [26,39], but at the cost of requiring much higher W_{rec} (at least 9 kWh/kg NH_4^+-N) than the biological systems, as microorganisms are not providing part of the required energy for the electrochemical reaction.

3.2. *Effects of the sulfuric acid solution properties on the ammonium recovery performance*

Most studies on the recovery of ammonium focus on process performance and may overlook the properties of the ammonium-enriched effluent. Hence, several influent sulfuric acid flowrates and concentrations were employed to assess their effects on the ammonium recovery performance and effluent characteristics (pH and TAN concentration). The baseline scenario, already showed in Table 1, is the combination of a recovery flowrate of 83 mL/d and a sulfuric acid concentration of 0.187 M. Two additional flowrates (60 and 40 mL/d corresponding to 3.3 and 5.0 days of hydraulic residence time) and two additional concentrations (0.140 and 0.093 M) were tested in two independent sets of experiments while maintaining all the other operational conditions previously employed (Fig. 3). For each condition, two reactors were used in parallel, and the results of their operation are summarized in Figs. S3 and S4 and Tables S2 and S3.

Theoretically, decreasing the recovery flowrate and the sulfuric acid concentration should have a similar effect since less protons are entering the recovery chamber. Decreasing the flowrate from 83 to 40 mL/d was observed to produce a slight decrease in E_{rem}, from 65 % to 55 % (Fig. 3A), and in R_{rem}, decreasing 20 % from the baseline case (Fig. 3B). The same trend was observed with E_{rec} and R_{rec} with small declines in the efficiency and 27 % decrease in the rate, whereas a similar behaviour

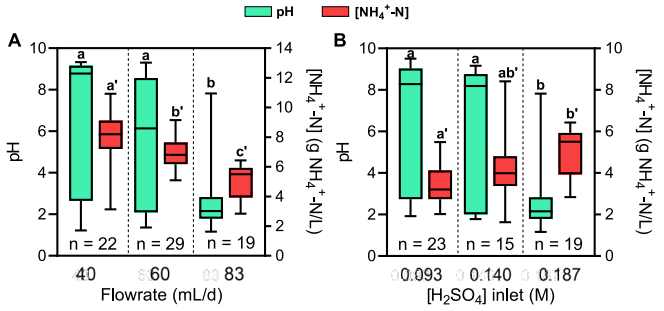

Fig. 5. Dispersion of pH and TAN concentration values with different recovery flowrates (A) and influent concentrations (B). Boxes represent median values with their correspondent 25 and 75 percentiles, bars show the minimum and maximum values, different letters above bars indicate significant differences among treatments and *n* describes the number of samples used in each dataset.

was seen when the concentration of sulfuric acid was decreased from 0.187 to 0.140 M. However, a sudden increase for both parameters was achieved at the lowest concentration of 0.093 M. In any case, when decreasing the acid concentration, the recovery efficiency and rates decreased to 65 %, and 30 g NH_4^+-N/m^2/d.

These results show the acidic solution characteristics may limit the TAN recovery performance: the higher flowrate or the higher acid concentration, the higher the removal/recovery performance. There is a self-reinforcing cycle here: the higher the recovery, the lower the ammonium concentration in the cathode and, thus, higher the TAN transfer through the CEM. The best values linked to TAN recovery (E_{rec}, R_{rec} and W_{rec}) were achieved when operating at 83 mL/d and 0.187 M of sulfuric acid.

The current densities achieved in all the operating conditions oscillated in the range of 2.4 and 3.5 A/m^2 (Fig. 3C). The potential losses caused by the 10 Ω resistance used for the current monitorization caused a reverse correlation between the current density and the applied voltage: the higher the current density, the lower was the voltage applied in the system. W_{rem} and W_{rec} followed a reverse trend compared to the ammonium transfer rates (Fig. 3D). Therefore, the lowest W_{rec} values were attained at the base conditions of 83 mL/d and 0.187 M of sulfuric acid.

To characterize nature and properties of the recovered effluent at different operating conditions, the resulting molar ratio between ammonium and sulphate ions was calculated and represented vs. the pH in the recovery effluent (Fig. 4). It resulted in a sigmoidal shape for the flowrate (Fig. 4A) and the sulfuric acid experiments (Fig. 4B), which fitted consistently the profiles expected for the theoretical titrations of sulfuric acid employing ammonia as a titrant [40]. The pH values in the effluent were grouped in only two main ranges: one acidic (1.1–3.4) and one alkaline (7.2–9.5) with an abrupt pH change adopting the form of the inflexion point of the sigmoidal shape. This abrupt change was located around an ammonium/sulphate molar ratio of 2, which is consistent with the neutralization stoichiometry of sulfuric acid (each molecule requires two molecules of ammonia).

Fig. 5 shows the distribution of pH and ammonium concentrations achieved in the effluent at different sulfuric acid solution flowrates (Fig. 5A) and concentrations (Fig. 5B). The default parameters of 83 mL/d and 0.187 M of sulfuric acid were the tested condition with the highest recovery capability, achieved the most acidic conditions in the effluent, with 75 % of the datapoints lower than 2.9 of pH.

An increase in pH was observed when the flowrate decreased, being half of the values higher than 8.7 at 40 mL/d. Concomitantly, an increase in average pH was also observed at both concentrations lower than 0.187 M. These observations were consistent since the amount of inlet acidity correlates with the amount of ammonia molecules that can be converted into ammonium before pH rises.

Simultaneously, the ammonium concentrations increased at lower

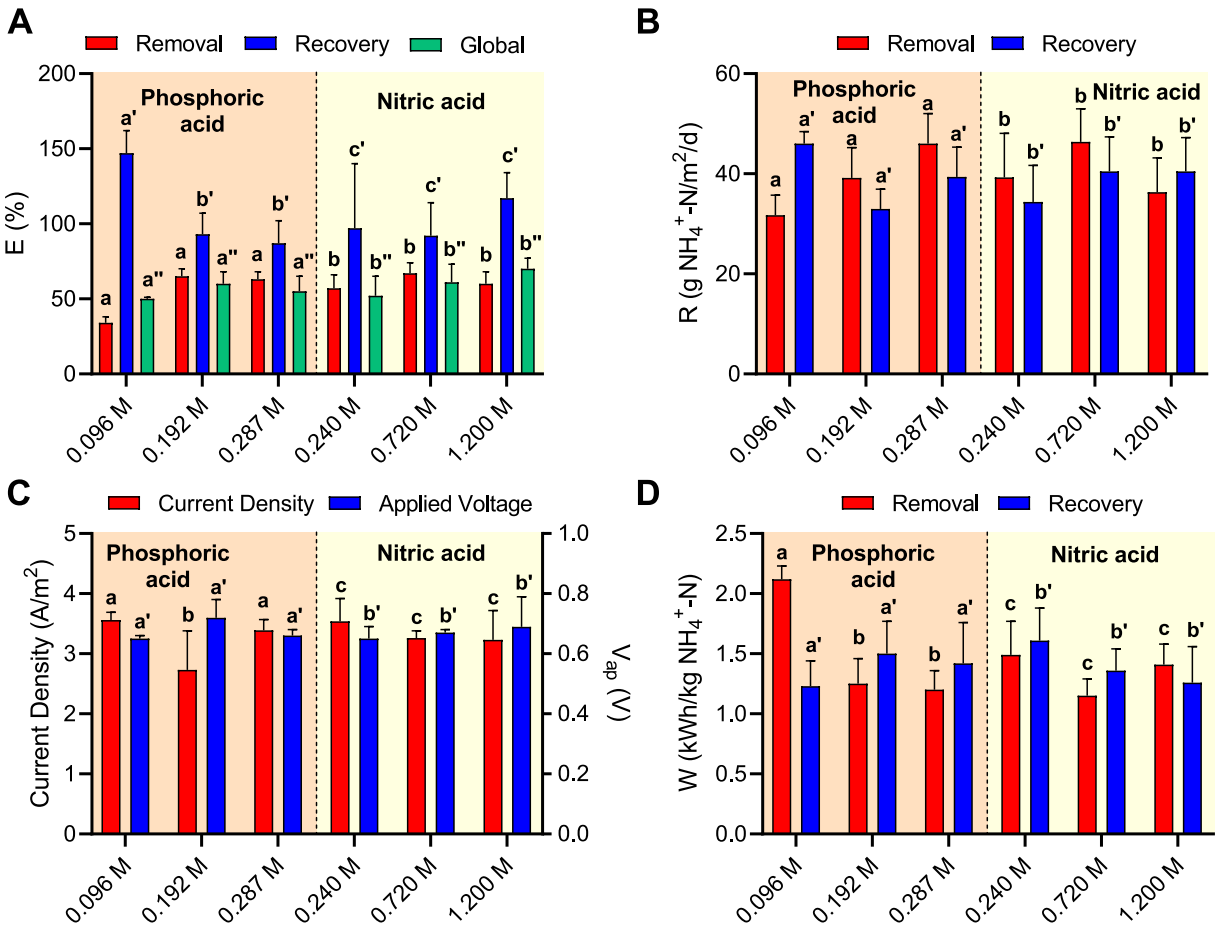

Fig. 6. Summary of the E_{rem}, E_{rec} (A), R_{rem}, R_{rec} (B), current density, V_{ap} (C), W_{rem} and W_{rec} (D) values with phosphoric and nitric acid in the recovery solution. Colour bars represent average values of all the selected experimental periods, error bars represent the standard deviation and different letters above bars indicate significant differences among each acid concentration according to Tukey's test ($p < 0.05$). The number of selected experimental periods for each condition was: H_3PO_4 – 0.096 M = 2, H_3PO_4 – 0.192 M = 6, H_3PO_4 – 0.287 M = 6, HNO_3 – 1.200 M = 6, HNO_3 – 0.720 M = 6 and HNO_3 – 0.240 M = 6.

recovery flowrates, going from 5.5 to 8.2 g NH_4^+-N/L at flowrates of 83 and 40 mL/d respectively since the lower flowrate, the more concentrated the effluent. A decline in ammonium concentration was observed at lower sulfuric acid concentrations, reaching a median value of 3.2 at the minimum concentration of 0.093 M. This finding corroborates that sulfuric acid concentration is a limiting factor for reaching high effluent TAN concentrations.

Moreover, these results show that flowrate and the inlet acid concentration can be manipulated to control either the effluent TAN concentration or pH. These conditions can benefit the application of the effluent as a sustainable nitrogen source for industrial biotechnological applications, avoiding possible inhibitions caused by high TAN concentrations or too alkaline conditions [8]. At an industrial level, controlling the recovery flowrate seems a more efficient approach for tuning the effluent TAN concentration rather than switching the acid concentration.

3.3. Effect of alternative acids in the recovered ammonium effluent

Sulfuric acid is a diprotic acid ($pKa_1 = -3.00$ and $pKa_2 = 1.92$) and has given successful results as a recovery agent. Phosphoric ($pKa_1 = 2.15$, $pKa_2 = 7.20$ and $pKa_3 = 12.38$) and nitric ($pKa = -1.30$) acids were studied as alternatives for being triprotic and monoprotic acids respectively. Besides that, phosphate and nitrate are anions frequently present in microbiological culture media, which broadens the range of applications for the recovered ammonium [41,42].

Figs. 6, S5 and S6 and Tables S4 and S5 show the results obtained at different acid concentrations at a fixed recovery flowrate of 83 mL/d. E_{rec} comprised between 50 and 70 % (Fig. 6A) similar to the results with sulfuric acid. Moreover, a positive correlation between the acid concentration and R_{rec} (Fig. 6B) corroborates that the ammonium assimilation capability of the recovery solution is a key performance parameter. The unexpected increase in recovery rate of the lowest phosphoric acid concentration tested, coupled to its surprisingly high recovery efficiency value (147 ± 15 %), can be explained by a possible absence of steady state in the system for this specific experiment.

All the R_{rec} were comprised between 30 and 50 g NH_4^+-N/m^2/d, in the range of those obtained with sulfuric acid. Regarding the nitric acid R_{rec}, there was no noticeable increase between the two highest concentrations tested (0.720 and 1.200 M) suggesting that the increase of the recovery assimilation capability can improve the ammonium transfer through the GDE up to a maximum value. Then, the system is limited by other step (i.e. ammonium transfer between anode and cathode or ammonium diffusion through the non-mixed catholyte).

Fig. 6C and D show that the current densities were maintained between 2.7 and 3.6 A/m^2 and the energy consumption values were comprised between 1.2 and 1.6 kWh/kg NH_4^+-N recovered, which are similar values than those with sulfuric acid. Nevertheless, the lowest value of 1 kWh/kg NH_4^+-N (0.187 M sulfuric acid) could not be achieved, remaining as the most energetically efficient configuration among the ones tested in this work. Fig. 7 shows the representation of the effluent pH values vs. the molar ratios between ammonium and the recovery agent (i.e. phosphoric or nitric acid). Regarding phosphoric acid, a clear agreement with the theoretical profile was observed (Fig. 7A). Being a

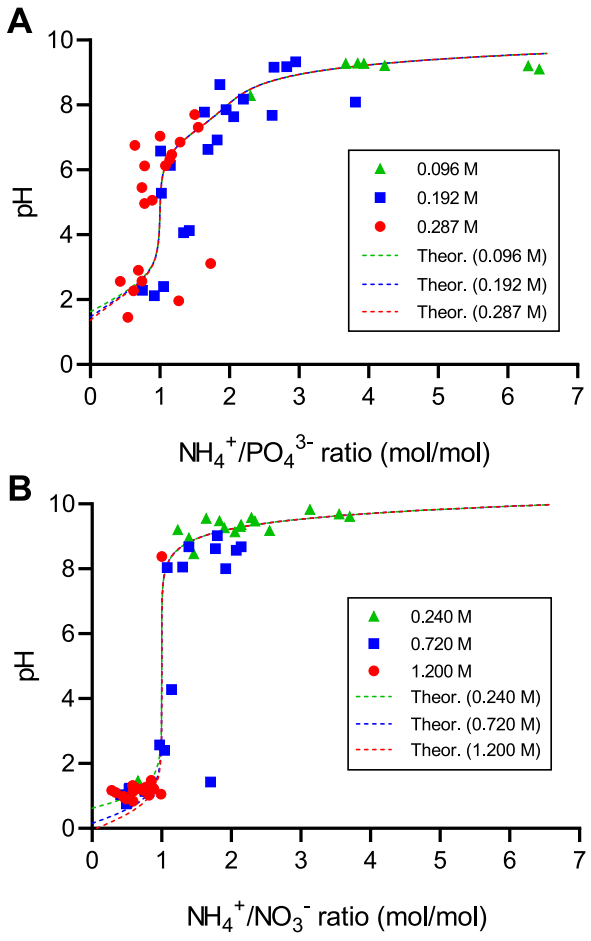

Fig. 7. pH of the recovery solution as a function of the NH_4^+/Acid molar ratio at different concentrations for phosphoric (A) and nitric (B) acids, compared to the theoretical pH value.

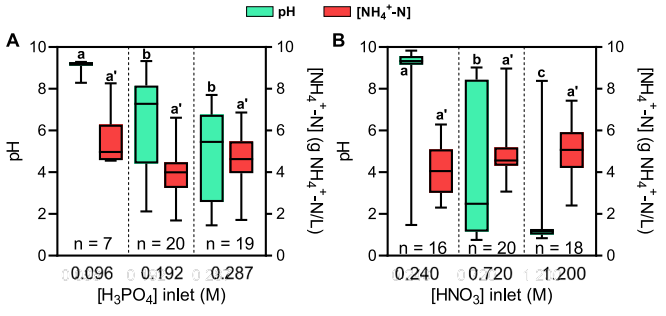

Fig. 8. pH dispersion and TAN concentration values for phosphoric (A) and nitric (B) acid concentrations as recovery agents. Boxes represent median values with their correspondent 25 and 75 percentiles, bars show the minimum and maximum values different letters above bars indicate significant differences among treatments and *n* describes the number of samples used in each dataset.

triprotic acid, the pH values adopted a broader dispersion in all the scale than in the case of sulfuric acid. The pH data was mainly observed in a small acidic range (1.4–3.2) and in a broader one located in the neutral/basic region (4.9–9.4), being the region between pH 3 and 5 the one with least data points. The maximum pH values were achieved from a ratio of 3 onwards when all phosphoric acid protons had reacted with the ammonia crossing the GDE. Fig. 8 shows the dispersion of the recovery parameters for each of the experiments. The dispersion of pH data for the phosphoric acid (Fig. 8A) shows a high prevalence of the intermediate areas (4–7) for the two highest phosphoric concentrations. The phosphoric acid concentration of 0.096 M resulted in pH values higher than 9.1 with a low dispersion. Overall, phosphoric acid is a more suitable recovery agent than sulfuric acid when the targeted pH needs to be comprised in the slightly acidic or neutral range and, thus, it would avoid an intensive pH adjustment as post-treatment.

Fig. 7B shows the results with nitric acid as recovery agent, where a higher split of pH was observed. The effluent datapoints were mainly located at pH lower than 1.5 when the molar ratio was lower than 1 in agreement with the number of protons present in the nitric molecule. However, a sudden increase to pH above 8 was observed once this ratio was exceeded. A high dispersion can be observed in the boxplots (Fig. 8B), particularly at 0.72 M. More than 75 % of the values were located at pH <1.3 at the highest nitric acid concentration, while the same percentage was located at pH >9.1 at the lowest one. In short, intermediate concentrations of recovery agent should be avoided when employing a monoprotic acid if a certain range of pH is targeted.

The recovered TAN slightly decreased at lower recovery agent concentrations (Fig. 8A and B), except for phosphoric acid at 0.96 M. Nevertheless, in most cases, effluent TAN was mainly comprised between 3 and 6 g NH_4^+-N/L. These values are lower than those obtained at low recovery agent flowrate (i.e. 8–9 g/L, see previous section). Hence, recovery agent flowrate as a manipulated parameter allows to fix either an effluent pH range or its TAN composition, whereas manipulating the recovery agent concentration will affect only the pH, with minor effects on TAN concentration.

Finally, the selection of the recovery agent should be based on its number of protons and its pKa values to obtain the desired effluent pH ranges. Combining all three design aspects, this work shows for the first time how to obtain custom-made ammonium-enriched effluents suitable for a wide variety of requirements.

3.4. *Exploring the potential of recovered ammonium for 3-HP production via K. phaffii*

As an example of the possible industrial application of the bio-electrochemically recovered TAN, this study also validates its utilisation as a nitrogen source for the microbial production of 3-HP via *K. phaffii* fermentation, a leading eukaryotic host organism for bioproducts over the last decade [43]. Recognized by the US Department of Energy (DOE) in 2004 and 2010 as a top value-added chemical from biomass, 3-HP is a vital building block for the production of commodity and specialty chemicals, including 1,3-propanediol, acrylamide, acrylic acid, and methyl acrylate [44].

The suitability of the recovered ammonium sulphate was compared to that of commercially available ammonium sulphate, a traditional nitrogen source in fermentation processes (Fig. 9). Employing the BESs described in this work, experimental tests were conducted achieving effluent pH levels of 2.1 and 8.8, which possessed ammonium to sulphate molar ratios of 2.9 and 3.2, respectively. In all the subsequent fermentations with *K. phaffii*, the pH of the employed effluent was adjusted to 5, and consistent initial ammonium concentrations were maintained across all experiments to ensure a stable nitrogen supply, essential for optimal microbial growth. On the other hand, sulphate concentrations varied according to the ratio of the collected sample. For comparison, the commercial ammonium sulphate control had the expected stoichiometric ratio of 2.

Comparable growth (optical density) and 3-HP production were observed across all conditions (Fig. 9). Flasks with ammonium sulphate recovered at pH = 6 produced 0.431 ± 0.04 g/L of 3-HP after 48 h, while those at pH = 2 produced 0.388 ± 0.057 g/L, and commercial ammonium sulphate yielded 0.401 ± 0.025 g/L. The variation in production was within an 8 % margin, demonstrating that recovered ammonium from BES is comparable to the commercial alternative and can be successfully integrated into the fermentation process.

Minimal media, such as YNB, are commonly employed for screening

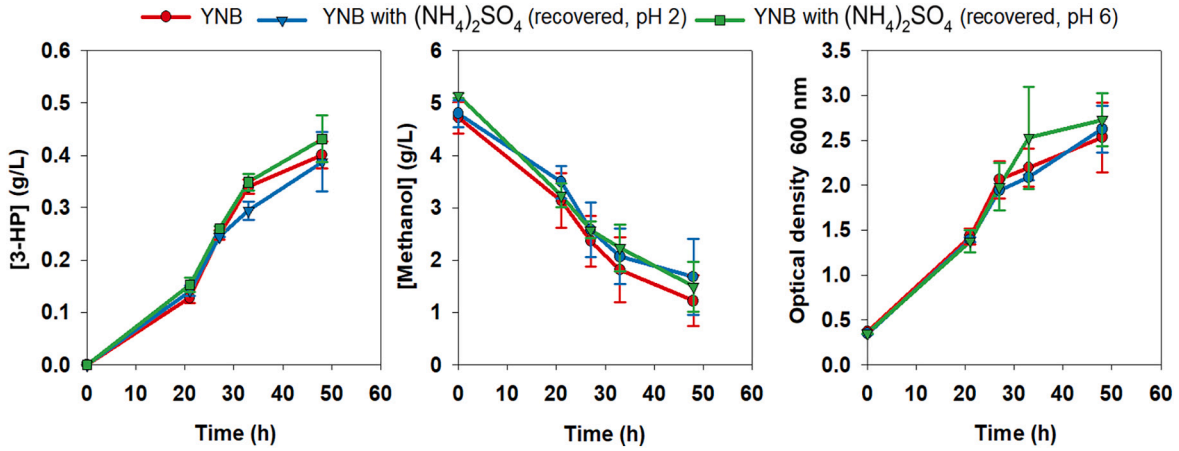

Fig. 9. Comparison of *K. phaffi* performance in YNB medium with commercial ammonium sulphate vs. ammonium sulphate recovered from BES at two different pHs.

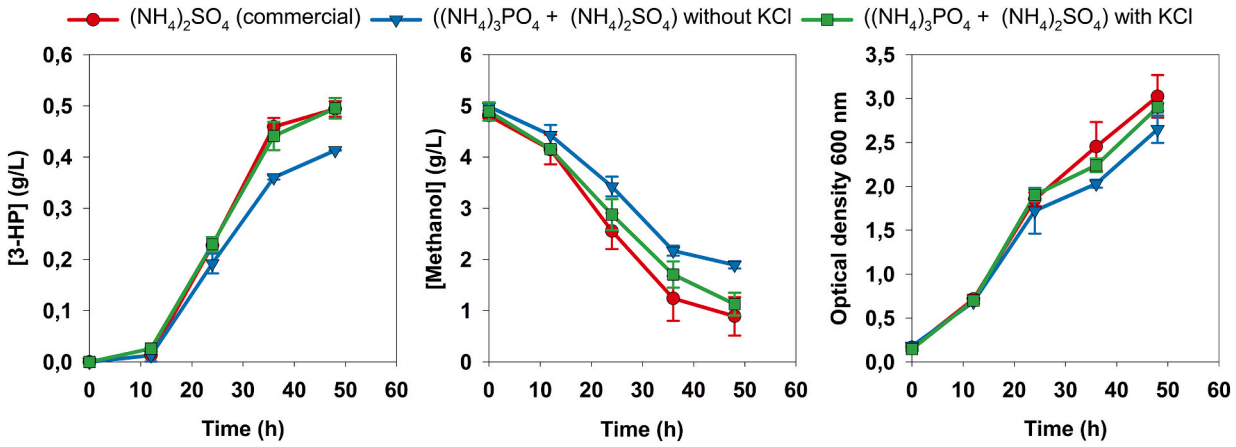

Fig. 10. Comparison of *K. phaffii* performance in YNB medium using commercial ammonium sulphate vs. a mixture of ammonium sulphate and ammonium phosphate recovered from BES with and without KCl.

microbial fermentation, providing insights into growth and basic metabolic functions [45]. While *K. phaffii* demonstrated good growth and 3-HP production using BES effluents with ammonium sulphate in YNB medium, switching to a more suitable growth medium with added nutrients is likely to enhance 3-HP production significantly. The pH in these experiments was adjusted to 5, which is optimal and widely used for *K. phaffii*, although the yeast can also thrive within a pH range of 3 to 7 [46]. Consequently, ammonium sulphate recovered from BES at neutral pH can be directly utilized with *K. phaffii*, offering flexibility for integration into microbial processes. This eliminates the need for pH adjustments, streamlining the overall procedure.

In the YNB medium, sulphate is the most abundant anion at 0.021 mol/L (2017 mg/L), followed by phosphate at 0.004 mol/L (380 mg/L). Since we have demonstrated that ammonium can be recovered together with different anions, including ammonium phosphate, we also aimed to substitute phosphate to optimize nutrient integration in the fermentation process. We employed a mixture of two different effluents derived from our bioelectrochemical cells to replace the essential nutrients ammonium, phosphate, and sulphate during the fermentation process, while maintaining the requisite concentration of ammonium for optimal growth. Given that phosphorus was supplied as potassium phosphate in the original YNB composition, we also investigated the necessity of incorporating an additional source of potassium to support cellular functions.

As demonstrated in Fig. 10, the combination of ammonium phosphate and ammonium sulphate effectively supported the growth and production of 3-HP in *K. phaffii*, yielding results comparable to commercial ammonium sulphate and potassium phosphate. However, the absence of potassium resulted in reduced growth and lower 3-HP production (0.413 g/L), underscoring the essential role of this element in optimizing metabolic performance. Notably, when supplemented with potassium chloride (KCl), this mixture achieved a 3-HP yield of 0.495 g/L after 48 h, closely matching the 0.494 g/L from commercial sources.

These findings highlight the high purity of recovered ammonium (99 % purity compared to other undesired ions such as sodium, nitrite, and chloride transferred from the catholyte) from the BES, ensuring compatibility with microbial growth and maintaining fermentation efficiency. Furthermore, this research demonstrates that ammonium recovered from BES can serve as a sustainable alternative to commercial nitrogen sources without compromising fermentation outcomes.

The results shown is this work open exciting avenues for integrating bioelectrochemically recovered ammonium into the current industrial context. Future studies should focus on the scalability of BES. Several aspects need to be carefully studied to assess the suitability of these systems at larger scales, such as reactor configuration; the ratio between volume and cross-sectional area; the electrode/membrane cost optimization, and the management of high volumes of the recovery acidic solution. Moreover, a thorough life-cycle assessment should be conducted, paying particular attention to the environmental advantages of incorporating recovered compounds from BES into various industrial processes to enhance the sustainability of bioprocessing.

4. Conclusions

The integration of a nickel-based GDE into a three-chamber, continuous-flow BES has proven to be a robust and efficient strategy for long-term ammonium recovery from wastewater. Consistently high ammonium removal and recovery rates, up to 47 g NH_4^+-N/m^2/d, were achieved while maintaining low energy consumption (~1.0 kWh/kg NH_4^+-N recovered) over prolonged operation. Systematic variation of recovery agent (nitric, phosphoric and sulfuric acids) concentration, and flow rate established effluent pH ranges (1−10) and ammonium concentrations (2.8–11.0 g NH_4^+-N/L) suitable for diverse applications. The results highlight a flexible and scalable framework for producing application-specific ammonium solutions, advancing the prospects for customizable, energy-efficient, and sustainable nitrogen recovery in wastewater treatment.

CRediT authorship contribution statement

David Fernández-Verdejo: Writing – original draft, Visualization, Methodology, Formal analysis, Data curation, Conceptualization. **Mariella Belén Galeano:** Writing – original draft, Visualization, Methodology, Formal analysis, Data curation, Conceptualization. **Zainab Ul:** Writing – original draft, Validation, Methodology, Data curation. **Deepak Pant:** Writing – review & editing, Methodology, Data curation. **Juan Antonio Baeza:** Writing – review & editing, Supervision, Software, Methodology, Formal analysis, Data curation, Conceptualization. **Albert Guisasola:** Writing – review & editing, Supervision, Resources, Project administration, Methodology, Funding acquisition, Data curation, Conceptualization.

Declaration of competing interest

The authors declare the following financial interests/personal relationships which may be considered as potential competing interests: Albert Guisasola reports financial support was provided by European Union. Juan Antonio Baeza reports financial support was provided by Government of Catalonia Agency for Administration of University and Research Grants. Albert Guisasola reports financial support was provided by Catalan Institution for Research and Advanced Studies. If there are other authors, they declare that they have no known competing financial interests or personal relationships that could have appeared to influence the work reported in this paper.

Acknowledgements

The authors acknowledge the support of the VIVALDI project that has received funding from the European Union's Horizon 2020 research and innovation programme under grant agreement 101000441. The authors from UAB are members of the GENOCOV research group (Grup de Recerca Consolidat de la Generalitat de Catalunya, 2021 SGR 515, www.genocov.com). Albert Guisasola acknowledges the funding from the ICREA Academia grant (2025–2029).

Appendix A. Supplementary data

Supplementary data to this article can be found online at https://doi.org/10.1016/j.cej.2025.172380.

Data availability

Data will be made available on request.

References

[1] R.B. Domingues, A.B. Barbosa, U. Sommer, H.M. Galvão, Ammonium, nitrate and phytoplankton interactions in a freshwater tidal estuarine zone: potential effects of cultural eutrophication, Aquat. Sci. 73 (2011) 331–343, https://doi.org/10.1007/s00027-011-0180-0.
[2] S.N. McCartney, N.A. Williams, C. Boo, X. Chen, N.Y. Yip, Novel isothermal membrane distillation with acidic collector for selective and energy-efficient recovery of ammonia from urine, ACS Sustain. Chem. Eng. 8 (2020) 7324–7334, https://doi.org/10.1021/acssuschemeng.0c00643.
[3] I. Kabdaslı, O. Tünay, İ. Öztürk, S. Yılmaz, O. Arıkan, Ammonia removal from young landfill leachate by magnesium ammonium phosphate precipitation and air stripping, Water Sci. Technol. 41 (2000) 237–240, https://doi.org/10.2166/wst.2000.0034.
[4] Y. Yao, L. Yu, R. Ghogare, A. Dunsmoor, M. Davaritouchaee, S. Chen, Simultaneous ammonia stripping and anaerobic digestion for efficient thermophilic conversion of dairy manure at high solids concentration, Energy 141 (2017) 179–188, https://doi.org/10.1016/j.energy.2017.09.086.
[5] R. Kanaan, P.H. Affonso Nóbrega, P. Achard, C. Beauger, Economical assessment comparison for hydrogen reconversion from ammonia using thermal decomposition and electrolysis, Renew. Sustain. Energy Rev. 188 (2023) 113784, https://doi.org/10.1016/j.rser.2023.113784.
[6] World Energy Outlook 2023, International Energy Agency IEA, 2023.
[7] N. Rahman, P.J. Forrestal, Ammonium fertilizer reduces nitrous oxide emission compared to nitrate fertilizer while yielding equally in a temperate grassland, Agriculture 11 (2021) 1141, https://doi.org/10.3390/agriculture11111141.
[8] X. Hu, J. Chu, S. Zhang, Y. Zhuang, X. Wu, H. Chen, Z. Lv, Z. Yuan, An alkaline pH control strategy for methionine adenosyltransferase production in Pichia pastoris fermentation, Biotechnol. Bioprocess Eng. 19 (2014) 900–907, https://doi.org/10.1007/s12257-014-0046-0.
[9] M.B. Galeano, M. Sulonen, Z. Ul, M. Baeza, J.A. Baeza, A. Guisasola, Bioelectrochemical ammonium recovery from wastewater: A review, Chem. Eng. J. 472 (2023), https://doi.org/10.1016/j.cej.2023.144855.
[10] K. Yang, M. Qin, The application of cation exchange membranes in electrochemical systems for ammonia recovery from wastewater, Membranes 11 (2021) 494, https://doi.org/10.3390/membranes11070494.
[11] C.I. Torres, R. Krajmalnik-Brown, P. Parameswaran, A.K. Marcus, G. Wanger, Y. A. Gorby, B.E. Rittmann, Selecting anode-respiring bacteria based on anode potential: phylogenetic, electrochemical, and microscopic characterization, Environ. Sci. Technol. 43 (2009) 9519–9524, https://doi.org/10.1021/es902165y.
[12] M. Rodríguez Arredondo, P. Kuntke, A. Ter Heijne, H.V.M. Hamelers, C.J. N. Buisman, Load ratio determines the ammonia recovery and energy input of an electrochemical system, Water Res. 111 (2017) 330–337, https://doi.org/10.1016/j.watres.2016.12.051.
[13] D. Pant, A. Singh, G. Van Bogaert, S. Irving Olsen, P. Singh Nigam, L. Diels, K. Vanbroekhoven, Bioelectrochemical systems (BES) for sustainable energy production and product recovery from organic wastes and industrial wastewaters, RSC Adv. 2 (2012) 1248–1263, https://doi.org/10.1039/C1RA00839K.
[14] N. Montpart, L. Rago, J.A. Baeza, A. Guisasola, Oxygen barrier and catalytic effect of the cathodic biofilm in single chamber microbial fuel cells, J. Chem. Technol. Biotechnol. 93 (2018) 2199–2207, https://doi.org/10.1002/jctb.5561.
[15] L. Rago, J.A. Baeza, A. Guisasola, Increased performance of hydrogen production in microbial electrolysis cells under alkaline conditions, Bioelectrochemistry 109 (2016) 57–62, https://doi.org/10.1016/j.bioelechem.2016.01.003.
[16] P. Kuntke, K.M. Śmiech, H. Bruning, G. Zeeman, M. Saakes, T.H.J.A. Sleutels, H.V. M. Hamelers, C.J.N. Buisman, Ammonium recovery and energy production from urine by a microbial fuel cell, Water Res. 46 (2012) 2627–2636, https://doi.org/10.1016/j.watres.2012.02.025.
[17] Z. Ul, M. Sulonen, J.A. Baeza, A. Guisasola, Continuous high-purity bioelectrochemical nitrogen recovery from high N-loaded wastewaters, Bioelectrochemistry 158 (2024) 108707, https://doi.org/10.1016/j.bioelechem.2024.108707.
[18] D. Hou, A. Iddya, X. Chen, M. Wang, W. Zhang, Y. Ding, D. Jassby, Z.J. Ren, Nickel-based membrane electrodes enable high-rate electrochemical ammonia recovery, Environ. Sci. Tech. 52 (2018) 8930–8938, https://doi.org/10.1021/acs.est.8b01349.
[19] M. Cerrillo, L. Burgos, E. Serrano-Finetti, V. Riau, J. Noguerol, A. Bonmatí, Hydrophobic membranes for ammonia recovery from digestates in microbial electrolysis cells: Assessment of different configurations, J. Environ. Chem. Eng. 9 (2021) 105289, https://doi.org/10.1016/j.jece.2021.105289.
[20] P. Zamora, T. Georgieva, A.T. Heijne, T.H.J.A. Sleutels, A.W. Jeremiasse, M. Saakes, C.J.N. Buisman, P. Kuntke, Ammonia recovery from urine in a scaled-up Microbial Electrolysis Cell, J. Power Sources 356 (2017) 491–499, https://doi.org/10.1016/j.jpowsour.2017.02.089.
[21] D. Losantos, M. Aliaguilla, D. Molognoni, M. González, P. Bosch-Jimenez, S. Sanchis, A. Guisasola, E. Borràs, Development and optimization of a bioelectrochemical system for ammonium recovery from wastewater as fertilizer, Cleaner Eng. Technol. 4 (2021) 100142, https://doi.org/10.1016/j.clet.2021.100142.
[22] X. Wu, O. Modin, Ammonium recovery from reject water combined with hydrogen production in a bioelectrochemical reactor, Bioresour. Technol. 146 (2013) 530–536, https://doi.org/10.1016/j.biortech.2013.07.130.
[23] O. Guerrero-Sodric, J.A. Baeza, A. Guisasola, Enhancing bioelectrochemical hydrogen production from industrial wastewater using Ni-foam cathodes in a microbial electrolysis cell pilot plant, Water Res. 256 (2024) 121616, https://doi.org/10.1016/j.watres.2024.121616.
[24] M. Qin, C. White, S. Zou, Z. He, Passive separation of recovered ammonia from catholyte for reduced energy consumption in microbial electrolysis cells, Chem. Eng. J. 334 (2018) 2303–2307, https://doi.org/10.1016/j.cej.2017.11.190.

[25] Z. Ul, M.B. Galeano, M. Sulonen, M. Baeza, J.A. Baeza, A. Guisasola, Electrochemical and bioelectrochemical ammonium recovery from N-loaded streams using a hydrophobic membrane, Bioelectrochemistry 166 (2025) 109013, https://doi.org/10.1016/j.bioelechem.2025.109013.
[26] G. Lee, D. Kim, J.-I. Han, Gas-diffusion-electrode based direct electro-stripping system for gaseous ammonia recovery from livestock wastewater, Water Res. 196 (2021) 117012, https://doi.org/10.1016/j.watres.2021.117012.
[27] I. Gonzalez-Salgado, C. Guigui, M. Sperandio, Transmembrane chemical absorption technology for ammonia recovery from wastewater: A critical review, Chem. Eng. J. 444 (2022) 136491, https://doi.org/10.1016/j.cej.2022.136491.
[28] H. Wu, C. Feng, L. Zhang, J. Zhang, D.P. Wilkinson, Non-noble metal electrocatalysts for the hydrogen evolution reaction in water electrolysis, Electrochem. Energy Rev. 4 (2021) 473–507, https://doi.org/10.1007/s41918-020-00086-z.
[29] Y. Ye, H.H. Ngo, W. Guo, Y. Liu, S.W. Chang, D.D. Nguyen, H. Liang, J. Wang, A critical review on ammonium recovery from wastewater for sustainable wastewater management, Bioresour. Technol. 268 (2018) 749–758, https://doi.org/10.1016/j.biortech.2018.07.111.
[30] Y. Jang, W. Lee, J. Park, Y. Choi, Recovery of ammonia from wastewater by liquid-liquid membrane contactor: a review, Membr. Water Treat. 13 (2022) 147–166, https://doi.org/10.12989/MWT.2022.13.3.147.
[31] D. Pinelli, A. Foglia, F. Fatone, E. Papa, C. Maggetti, S. Bovina, D. Frascari, Ammonium recovery from municipal wastewater by ion exchange: Development and application of a procedure for sorbent selection, J. Environ. Chem. Eng. 10 (2022) 108829, https://doi.org/10.1016/j.jece.2022.108829.
[32] J. Zhu, Q. Zhao, J. Wang, N. Li, M. Chen, X. Wang, Negative-pressure gas-diffusion electrode for effective ammonia recovery in bioelectrochemical systems, J. Clean. Prod. 414 (2023) 137641, https://doi.org/10.1016/j.jclepro.2023.137641.
[33] A. Ronen, W. Duan, I. Wheeldon, S. Walker, D. Jassby, Microbial attachment inhibition through low-voltage electrochemical reactions on electrically conducting membranes, Environ. Sci. Technol. 49 (2015) 12741–12750, https://doi.org/10.1021/acs.est.5b01281.
[34] F. Zhang, S. Cheng, D. Pant, G.V. Bogaert, B.E. Logan, Power generation using an activated carbon and metal mesh cathode in a microbial fuel cell, Electrochem. Commun. 11 (2009) 2177–2179, https://doi.org/10.1016/j.elecom.2009.09.024.
[35] J.A. Baeza, Advanced Direct Digital Control (AddControl): lessons learned from 20 years of adding control to lab and pilot scale treatment systems, in: ICA2022, 13th IWA Conference on Instrumentation. Control and Automation, Beijing, China, 2022.
[36] M. Cheng, C. Zhang, A. Guisasola, J.A. Baeza, Evaluating the opportunities for mainstream P-recovery in anaerobic/anoxic/aerobic systems, Sci. Total Environ. 912 (2024) 168898, https://doi.org/10.1016/j.scitotenv.2023.168898.
[37] K. Yang, M. Qin, Enhancing selective ammonium transport in membrane electrochemical systems, Water Res. 257 (2024) 121668, https://doi.org/10.1016/j.watres.2024.121668.
[38] N. Wang, Y. Feng, Y. Li, L. Zhang, J. Liu, N. Li, W. He, Effects of ammonia on electrochemical active biofilm in microbial electrolysis cells for synthetic swine wastewater treatment, Water Res. 219 (2022) 118570, https://doi.org/10.1016/j.watres.2022.118570.
[39] X. Wang, S. Im, B. Jung, J. Wu, A. Iddya, Q.-R.A. Javier, M. Xiao, S. Ma, S. Lu, B. Jaewon, J. Zhang, Z.J. Ren, C.T. Maravelias, E.M.V. Hoek, D. Jassby, Simple and low-cost electroactive membranes for ammonia recovery, Environ. Sci. Technol. 57 (2023) 9405–9415, https://doi.org/10.1021/acs.est.3c01470.
[40] D.C. Harris, Quantitative chemical analysis, 7. ed, print, Freeman, New York, 2007, p. 2.
[41] W. Zhang, J. Sinha, M.M. Meagher, Glycerophosphate as a phosphorus source in a defined medium for Pichia pastoris fermentation, Appl. Microbiol. Biotechnol. 72 (2006) 139–144, https://doi.org/10.1007/s00253-005-0238-9.
[42] J. Böllmann, M. Martienssen, Comparison of different media for the detection of denitrifying and nitrate reducing bacteria in mesotrophic aquatic environments by the most probable number method, J. Microbiol. Methods 168 (2020) 105808, https://doi.org/10.1016/j.mimet.2019.105808.
[43] B.G. Ergün, K. Laçın, B. Çaloğlu, B. Binay, Second generation Pichia pastoris strain and bioprocess designs, Biotechnol. Biofuels 15 (2022) 150, https://doi.org/10.1186/s13068-022-02234-7.
[44] T. Werpy, G. Petersen, Top Value Added Chemicals From Biomass: Volume I – Results of Screening for Potential Candidates From Sugars and Synthesis Gas, 2004, https://doi.org/10.2172/15008859.
[45] C.B. Matthews, A. Kuo, K.R. Love, J.C. Love, Development of a general defined medium for *Pichia pastoris*, Biotechnol. Bioeng. 115 (2018) 103–113, https://doi.org/10.1002/bit.26440.
[46] O. Cos, R. Ramón, J.L. Montesinos, F. Valero, Operational strategies, monitoring and control of heterologous protein production in the methylotrophic yeast Pichia pastoris under different promoters: a review, Microb. Cell Fact. 5 (2006) 17, https://doi.org/10.1186/1475-2859-5-17.